COMPDYN 2015
5th ECCOMAS Thematic Conference on
Computational Methods in Structural Dynamics and Earthquake Engineering
M. Papadrakakis, V. Papadopoulos, V. Plevris (eds.)
Crete Island, Greece, 25–27 May 2015

EXPERIMENTAL AND NUMERICAL ANALYSIS ON THE CYCLIC BEHAVIOR OF BRIDGE PIERS WITH AND WITHOUT CFRP RETROFIT

Pedro Delgado[1], Frutuoso Sousa[1], Patrício Rocha[1], António Arêde[2], Nelson Vila Pouca[2], Aníbal Costa[3], and Raimundo Delgado[2]

[1] Instituto Politécnico de Viana do Castelo
Apartado 574, 4901-908 Viana do Castelo, Portugal
pdelgado@estg.ipvc.pt, frutuososousa@ipvc.pt, procha@estg.ipvc.pt

[2] Universidade do Porto - Faculdade de Engenharia
R. Dr. Roberto Frias, s/n 4200-465 Porto, Portugal
aarede@fe.up.pt, nelsonvp@fe.up.pt, rdelgado@fe.up.pt

[3] Universidade de Aveiro
Campus Universitário de Santiago, 3810-193 Aveiro, Portugal
acosta@civil.ua.pt

Keywords: RC hollow piers, numerical analysis, experimental tests, retrofit strategies

Abstract. *The main objective of this paper is to evaluate the cyclic behavior of RC hollow piers, with and without with CFRP retrofit, by comparison of experimental tests results with structural numerical modeling. The retrofit techniques aim to increase the shear strength and the ductility capacity through the establishment of principles and strategies applied in an experimental cyclic campaign of RC hollow piers, carried out in the Laboratory for Earthquake and Structural Engineering (LESE) of the Faculty of Engineering of University of Porto (FEUP). The evaluation and calibration of the efficiency of several retrofit solutions is also performed. The numerical simulations are carried out using two different methodologies: (i) fiber model and (ii) damage model. The fiber models based in a finite element discretiztion with non-linear behavior distributed along the elements length and cross-sectional area, while the damage model is supported on refined finite element (FE) meshes, with high complexity and detail levels in the constitutive laws defined for both concrete and steel. The concrete is simulated with a continuum damage model where several applications for bridges with hollow section piers can be found at Faria et al. [1]. Results of the experimental campaign allow to discuss and conclude about the efficiency of each numerical method, namely regarding the shear strength and the ductility capacity assessment.*

1 INTRODUCTION

Hollow piers have large section dimensions, with reinforcement bars spread along both wall faces, and unlike common solid section columns, quite often the shear effect has great importance on the pier behavior. Thus, special attention should be given to this issue when the numerical assessment and retrofit of such type of section piers is envisaged. In line with this concern, an experimental campaign has been carried out at LESE – FEUP (Laboratory of Earthquake and Structural Engineering of the Faculty of Engineering of University of Porto), on a set of RC piers. The test setup characteristics and more detailed results are available in previous reports [2-5]. This set of specimens was based on square piers tested at the Laboratory of Pavia University, Italy [6, 7], consisting on hollow section RC piers with 450mm x 450mm exterior dimensions and 75mm thick walls, and is being tested in order to understand the influence of the cross section geometry of rectangular hollow piers on the cyclic behavior, bearing in mind the purpose of assessing retrofitting solutions.

2 PROTOTYPES

Ten prototypes with square and rectangular hollow section (see Table 1 and Figure 1) were tested with different transverse reinforcement details, namely: piers N2, N3 and N4 - simple stirrups with 2 legs (representative of the old bridge construction); piers N5 - more detailed transverse reinforcement with 2 legs, with EC8 type, and piers N6 - also detailed stirrups (like piers N5), but with 4 legs (twice cross section area of transverse reinforcement).

Piers	Square Section	Rectangular Section
2ª Construction series	PO1-N2	PO2-N2
	PO1-N3	PO2-N3
3ª Construction series	PO1-N4	PO2-N4
	PO1-N5	PO2-N5
	PO1-N6	PO2-N6

Table 1: Construction series.

The unconfined concrete compressive strength (f_c) is 28 MPa and the longitudinal and transversal reinforcement yielding strengths (f_{sy} and f_{swy}) are represented in Table 2. The model schemes shown in Figure 1a correspond to ¼ scale representations of bridge piers with square and rectangular hollow section, herein referred to as PO1 and PO2, respectively. Instrumentation to measure curvature and shear deformations was included along the pier height, because important shear deformations were expected in these tests. The LVDT configuration used in both specimens is shown in Figure 1b.

Designation	Geometry	Concrete	Long. Reinf.		Transv. Reinf.		
		f_c (MPa)	area	f_{sy} (MPa)	ϕ (mm)	f_{swy} (MPa)	type
PO1-N2	Square	28	40ϕ8	435	2.6	440	2 legs
PO1-N3	Square	28	40ϕ8	435	2.6	440	2 legs
PO1-N4	Square	28	40ϕ8	560	2.6	440	2 legs
PO1-N5	Square	28	40ϕ8	560	2.6	440	2 legs (EC8)
PO1-N6	Square	28	40ϕ8	560	2.6	440	4 legs (EC8)
PO2-N2	Rectangular	28	64ϕ8	435	2.6	440	2 legs
PO2-N3	Rectangular	28	64ϕ8	435	2.6	440	2 legs
PO2-N4	Rectangular	28	64ϕ8	560	2.6	440	2 legs
PO2-N5	Rectangular	28	64ϕ8	560	2.6	440	2 legs (EC8)
PO2-N6	Rectangular	28	64ϕ8	560	2.6	440	4 legs (EC8)

Table 2: Hollow piers characteristics.

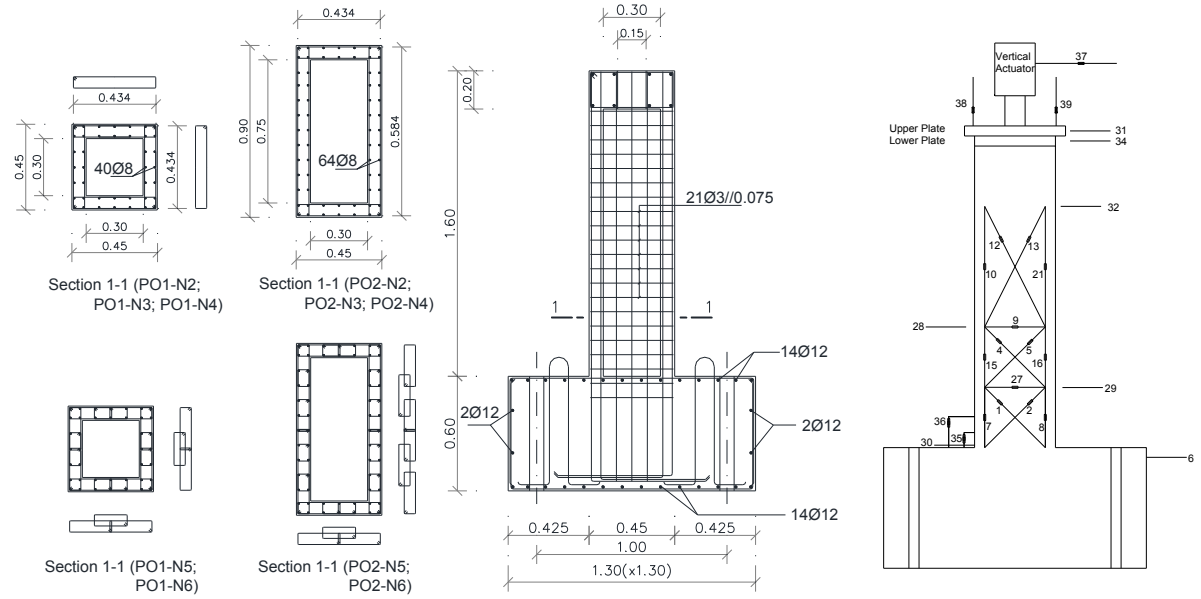

a) b)

Figure 1: Hollow RC piers: a) geometry of specimen and b) lateral LVDT layout.

To define the values of Table 3, simple calculation were carried out for the cross section to compute the flexural capacity, while to evaluate the shear capacity the methodology suggested by Priestley [8] was adopted, usually referred in the bibliography as original UCSD shear model [9], being the shear strength (V_d) obtain for these piers through equation 1:

$$V_d = V_c + V_s + V_p \quad (1)$$

where V_c, V_s and V_p are the shear force components accounting, respectively, for the nominal strength of concrete (which depends on the pier displacement ductility), the transverse reinforcement shear resisting mechanism and the axial compression force. These values were obtained for an axial load of 250 kN (except pier PO2-N3 with 440kN) that corresponds to a normalized axial force of 0.08 and 0.05, respectively for the square and rectangular pier cross sections [2].

Designation	Geometry	Flexural Capacity (kN)		Shear Capacity (kN)	
		yielding	ultimate	ductility of 2	ductility of 8
PO1-N2	Square	155	180	170	105
PO1-N3	Square	155	180	170	105
PO1-N4	Square	185	215	170	105
PO1-N5	Square	185	215	170	105
PO1-N6	Square	185	215	220	160
PO2-N2	Rectangular	230	265	170	105
PO2-N3	Rectangular	255	290	200	135
PO2-N4	Rectangular	280	320	170	105
PO2-N5	Rectangular	280	320	170	105
PO2-N6	Rectangular	280	320	220	160

Table 3: Flexural and shear capacities.

To define the cyclic behavior of piers for experimental tests, was followed a displacement history with three cycles repeated for each range, represented in Table 4.

Displacement. (mm)	***Drift* (%)**
1	0,07
3	0,21
5	0,35
10	0,70
4	0,28
14	1,00
17	1,20
7	0,50
25	1,80
30	2,10
33	2,40
40	2,90
45	3,20

Table 4: Displacement history of experimental tests.

3 RESULTS OF ORIGINAL PIERS

The damage of flange walls (face north and south, which are the perpendicular to the applied force) exhibited mainly horizontal cracking along the pier height. On the other hand it becomes clear that the pier webs (lateral faces east and west) were the most damaged zones of all specimens, exhibiting inclined cracking and concrete spalling on extensive zones, Figure 2. Generally, these damage patterns are associated with shear mechanisms, reveling insufficient shear capacity provide by transverse reinforcement. However, some square piers have shear capacity slightly above the flexural capacity (see Table 5), which have resulted on a mixed collapse mechanism, bending/shear.

(a) square – flange (b) square – web (c) rectangular – flange (d) rectangular – web

Figure 2: Typical final damage on the webs and flange for square and rectangular cross sections piers.

In the Table 5 is presented a summary of shear and flexural capacities, the values of experimental results, as well as the collapse mechanism. The definition of collapse displacement corresponds to the value when the horizontal force applied to the pier reached 80% of the maximum force. For almost all the piers the shear capacity is clearly below the flexural capacity, being the maximum experimental force closer to the numerical estimation of shear strength, although in some cases the experimental response has reached a peak force slightly above the expected values.

Piers	Numerical Flexural Cap. (kN)	Numerical Shear Cap. (kN)	Experimental Max. Force (kN)	Experimental Collapse Displ. (mm)	Collapse mechanism
PO1-N2	155 / 180	170 / 105	130	33	Flexural / Shear
PO1-N3	155 / 180	170 / 105	130	33	Flexural / Shear
PO1-N4	185 / 215	170 / 105	170	25	Shear
PO1-N5	185 / 215	170 / 105	170	25	Shear
PO1-N6	185 / 215	220 / 160	210	30	Shear
PO2-N2	230 / 265	170 / 105	190	25	Shear
PO2-N3	255 / 290	200 / 135	220	25	Shear
PO2-N4	280 / 320	170 / 105	190	30	Shear
PO2-N5	280 / 320	170 / 105	200	30	Shear
PO2-N6	280 / 320	220 / 160	250	40	Shear

Table 5: Resume of forces and collapse mechanism for square and rectangular cross section piers.

For illustration purpose the cyclic response of two piers (PO2-N5 and PO2-N6) are shown in Figure 3, where it is also included the shear capacity lines for both piers (equation 1). In comparison with PO2-N5, a significant improvement was observed in the cyclic response of pier PO2-N6, due to the effect of doubling the transverse reinforcement. This pier has reached the expected level force determined numerically, but, not enough to achieve the strength level needed to yielding of the longitudinal reinforcement. However, the residual strength level obtained at the end of this experimental test is only slightly lower than the maximum peak value of the experimental test PO2-N5, those values occurring for a displacement, relative to PO2-N5, almost double, as demonstrated in Figure 3. Since both piers have the same maximum flexural force of about 300kN, associated with the yielding of the longitudinal reinforcement, premature shear failure was found for both piers, PO2-N5 and PO2-N6.

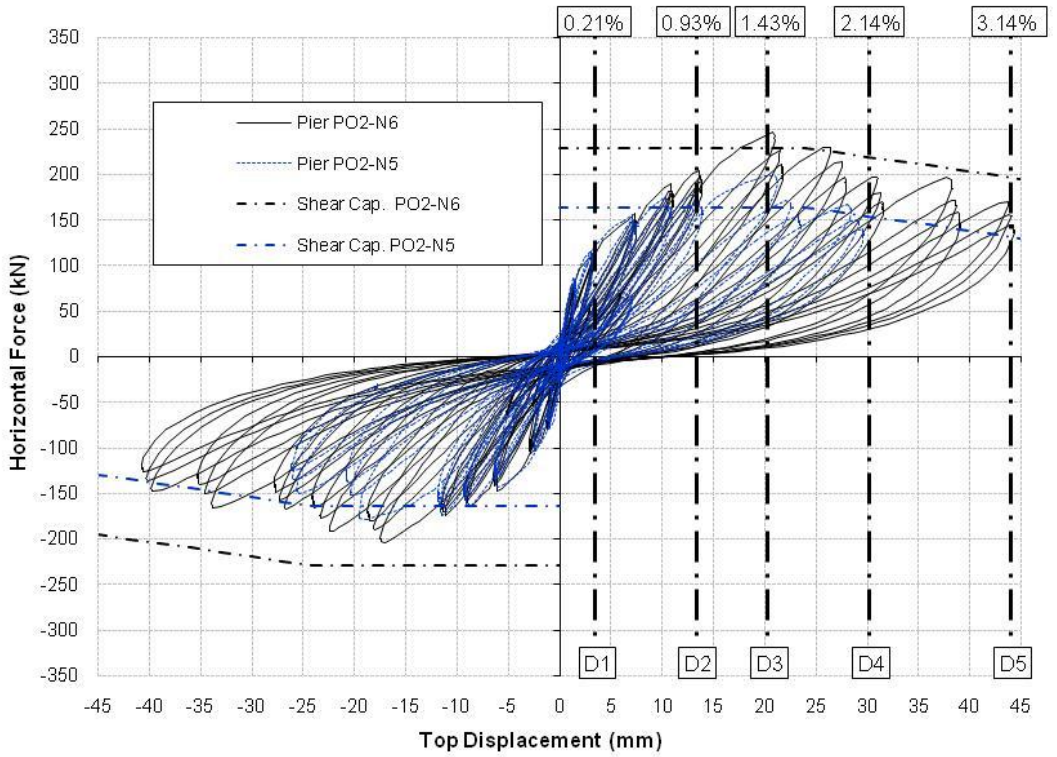

Figure 3: Experimental results comparison - PO2-N5 vs PO2-N6

4 RESULTS OF RETROFIT SOLUTIONS

The main objective of reinforcement techniques are improve the strength and ductility of structural elements. Therefore, the specimens used in previous experimental tests will be subject to a retrofit process in order to evaluate the increase of shear strength and ductility capacities of the retrofit solutions.

4.1 Retrofit process

After the original specimen cyclic tests, piers were repaired and retrofitted by an external contractor (S.T.A.P.) according to the following steps: 1) delimitation of the repair area; 2) removal and cleaning of the damaged concrete; 3) inside retrofit with transversal steel bars; 4) alignment or replacement of the longitudinal rebars; 5) application of formwork and new concrete (Microbeton, a pre-mixed micro concrete, modified with special additives to reduce shrinkage in the plastic and hydraulic phase); 6) outside retrofit with the CFRP sheets. In order to provide a general idea of the pier damage and of the retrofit process, the following pictures show the piers during repair and after retrofit with CFRP sheet jacketing (Figure 4). The inside retrofit with transversal steel bars (only for pier PO2-N3) was designed taking in account the feasibility for future real retrofits; such bars were concentrated at the bottom, in correspondence with the outer CFRP jackets, for improving the plastic hinge confinement.

In order to design the outside shear retrofit with CFRP jackets, the methodology suggested by Priestley [8, 9] was adopted to evaluate the thickness of the rectangular hollow pier jacket for increasing the shear strength above the maximum flexural force while keeping the initial

section conditions. According to this methodology the shear strength can be conveyed by equation 2:

$$V_d = V_c + V_s + V_p + V_{sj} \quad (2)$$

where V_c, V_s and V_p are the shear force components accounting, respectively, for the nominal strength of concrete, the transverse reinforcement shear resisting mechanism and the axial compression force; the term V_{sj} corresponds to the possible retrofit contribution with CFRP or metal jackets and can be estimated according to equation 3:

$$V_{sj} = \frac{A_j}{s} f_j \cdot h \cdot \cot\theta \quad (3)$$

where h is the overall pier section dimension parallel to the applied shear force, f_j is the adopted design jacket stress, A_j is the transverse section area of the jacket sheets spaced at distance s and inclined of the angle θ relative to the member axis.

4.2 Experimental results of PO2-N5-R1 and PO2-N5-R2

For PO2-N5-R1 pier, one strip layer of CFRP sheet with 0,177 mm thick and 100 mm wide was applied. The spacing was 100 mm along the pier height in order to increase the shear capacity, but it was decided to leave a 100 mm distance at the base in order to analyze the available ductility of the pier if shear collapse mechanism was avoided [2].

When it reached 2.5% drift, occurred a premature rupture of CFRP sheet in west side, as can be seen from in Figure 4. As the purpose of this experimental test was the evaluation the flexural behavior of pier, the test was interrupted and the pier was conveniently retrofitted in all its height to avoid any weakness to the shear effect.

a) east side b) south side c) north side d) west side

Figure 4: Final damage of pier PO2-N5-R1, for 2,5% drift.

After this second retrofit with the objective to prevent collapse mechanism by shear, the pier was renamed to PO2-N5-R2. However, when it reached 2.9% drift, the four strips of CFRP closest to the bottom of the pier suffered a sudden rupture in west side, causing a collapse mechanism of pier by shear effect. In Figure 5, it can be observed the fiber and concrete damage, as well as the cracks that appear during the test.

By analyzing the results depicted in Figure 6, it can be concluded that the retrofit executed showed an unsatisfactory behavior, particularly in terms of maximum displacement achieved. However, this retrofit presented a higher strength capacity in compared to the original pier. But, indeed, this retrofit failed to prevent the shear collapse mechanism [2].

a) east side b) south side c) north side d) west side

Figure 5: Final damage of pier PO2-N5-R2, for 2,9% drift.

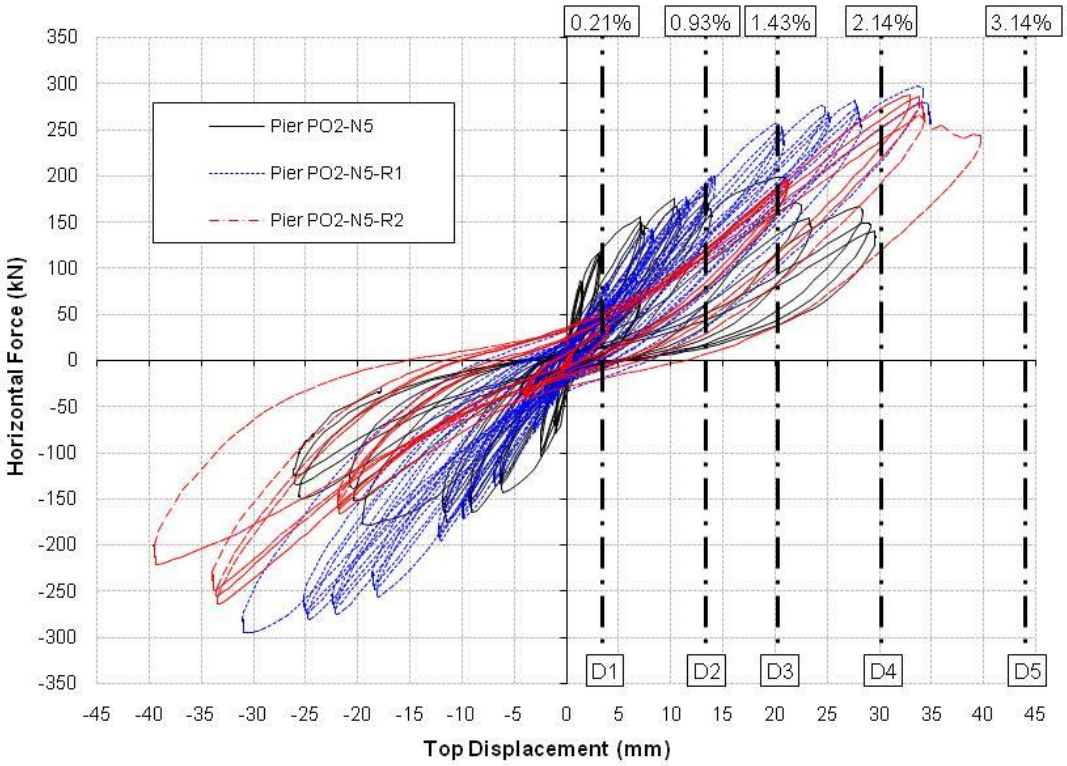

Figure 6: Experimental results comparison - PO2-N5 vs PO2-N5-R1 vs PO2-N5-R2.

4.3 Experimental results of PO2-N6-R1

For this specimen, one strip layer of CFRP sheet was used, which was 0.177 thick, 100 mm wide and spaced at 100 mm along the pier height in order to increase the shear capacity. As considered in pier PO2-N5-R1, it was decided to leave a 100 mm distance at the base in order to analyze the available ductility of the pier if shear collapse mechanism was avoided.

When 3.0% drift was achieved, corresponding to 45 mm of top pier displacement, the second strip of CFRP (counting for the bottom) broke up in the northeast corner. In the subsequent cycles, broke up the 3º, 4º, 5º and 6º fiber strips, in ascending order, in the same

corner as the second strip, Figure 7. After the abrupt rupture of the fibers, the pier lose the concrete confinement, causing the desegregation of the material on the east side wall pier, as can be seen in Figure 7. Finally, after the experimental test has been stopped, high deterioration of the concrete and some buckling phenomena of longitudinal rebars were observed [10].

a) east side b) south side c) north side d) west side

Figure 7: Final damage of pier PO2-N6-R1, for 3.0% drift.

Although the failure mechanism of the pier PO2-N6-R1 was achieved by shear mechanism, it can be observed from Figure 8 that the maximum strength increased about 50% in comparison with the original pier (PO2-N6).

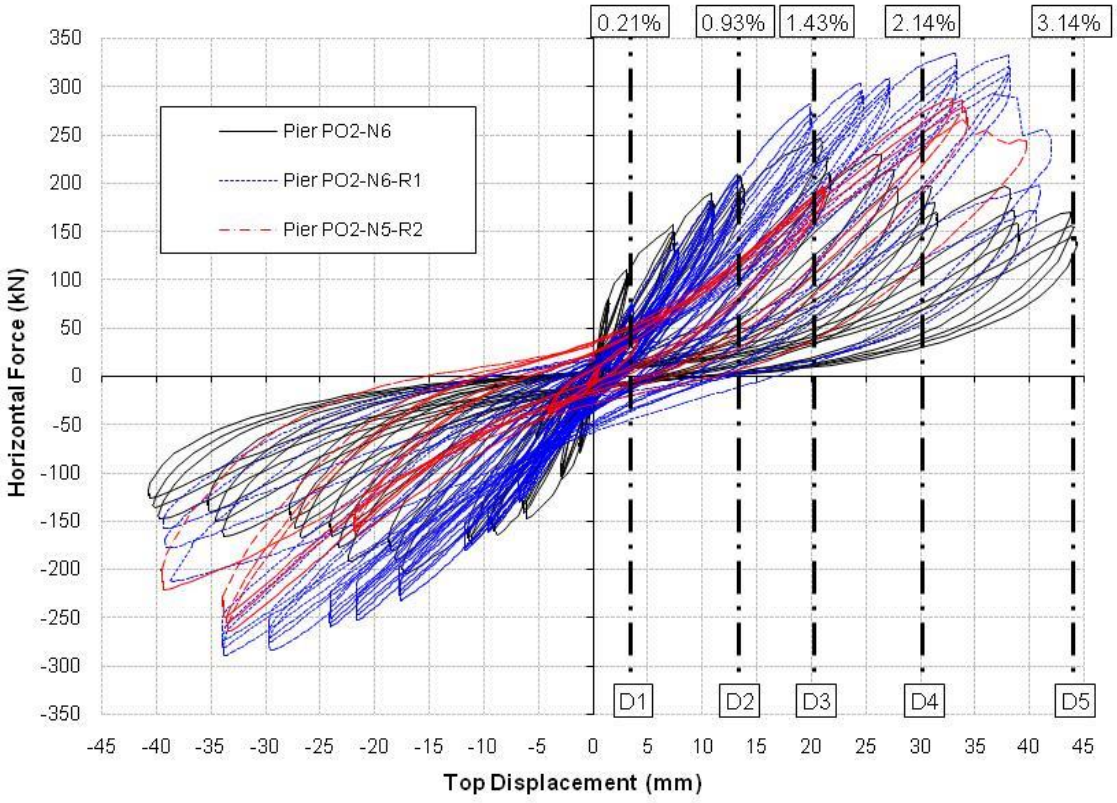

Figure 8: Experimental results comparison - PO2-N6 vs PO2-N6-R1 vs PO2-N5-R2.

Therefore, a higher bending contribution was obtained in the pier behavior (in comparison with the original pier), despite the shear deformation effects that occurred during the test. But in terms of displacement, this pier retrofit just have reached the ductility between 3 and 4, due to CFRP strips failed to accommodate the pier web deformation and broken.

Also in Figure 8, it can be observed an increase of the maximum force achieved for the same displacement level exceeding 50 kN in relation to PO2-N5-R1. These differences may be due to the difference in amount of transverse reinforcement, because the retrofit of both piers was exactly the same. In fact, as already mentioned, N6 piers have the double area of transverse reinforcement in relation to N5.

5 NUMERICAL ANALYSIS

After the interpretation of the results obtained by experimental tests, will be carried a numerical analysis of pier PO2-N6 to explain all phenomena involved, namely the failure mechanisms by shear and bending. The first numerical tool used to perform these analyzes was the fiber method, the freeware Seismostruct [11]. The numerical analyzes were performed with the displacement history used in the experimental tests (Table 4) and with the characteristics and properties of piers shown in Table 2.

In Figure 9 are shown the results of experimental tests and numerical PO2-N6, with and without retrofit in a diagram force - displacement.

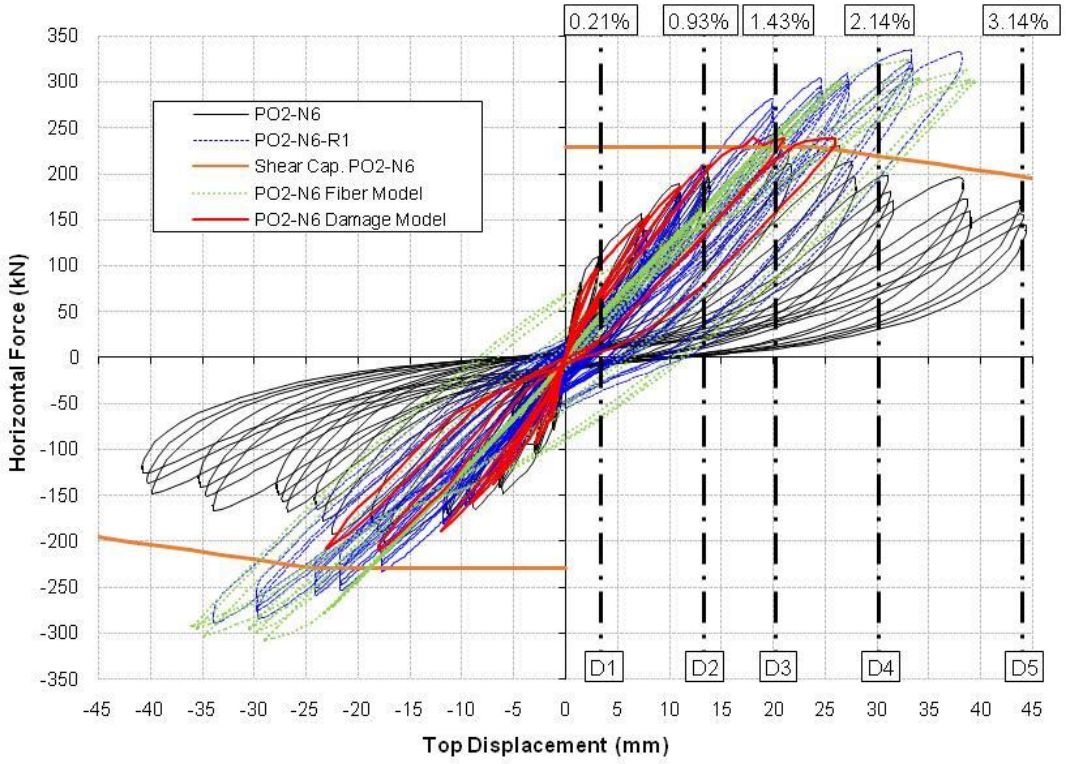

Figure 9: Experimental results vs Numerical results

The difference between the results of the fiber model and the experimental test of pier PO2-N6 is due to a limitation of this numerical model to simulate the shear effects. Namely, the fiber model of Seismostruct [11] assumes that the pier is governed by bending behavior, which leads to a maximum forces achieved similar to those obtained in the experimental test

of the retrofit pier (PO2-N6-R1), once it is capable to explore a higher bending component due to the CFRP strips retrofit. This numerical model does not consider the deformation and stiffness degradation from shear effects, which is quite relevant for the piers behavior when inclined cracks occurs in its webs. This inability to consider the shear effect leads to maximum forces of fiber model (in Figure 9) similar to those shown in Table 5 for flexural capacity (about 320 kN) [10].

The deformation and strength mechanisms associated to shear are related to the concrete tensile behavior [5]. The damage model [1] makes use of "effective stress tensors" decomposed in compression and tensile stresses that lets you explore the deformation and stiffness degradation by shear. As can be seen in figure 9, the damage model results show a good approximation to the experimental test of pier PO2-N6, with a quite accurate simulation of the shear effects.

6 CONCLUSIONS

The comparison of the experimental tests of original piers, PO2-N5 with PO2-N6, allowed to confirm the importance of transverse reinforcement to control the shear deformation. Despite rupture of both piers has been obtained by a shear mechanism, the solution with the twice transverse reinforcement achieved a significant increase in the maximum strength and maximum displacement, exploring a higher bending component.

The comparison of original and retrofit piers, allow concluding that this retrofit technique increases the achieved maximum strength, with similar values of those determined by simple expressions of the bending capacity.

After the tests of retrofitted piers was observed that was difficult to achieve high levels of ductility, due to the difficulty of the CFRP sheets to follow the piers web deformation. This resulted in the collapse of the CFRP sheets to ductility levels below 4.

The numerical analysis were quite useful for helping to understand some phenomena observed in the experimental tests, as for example the formation of failure modes. Through the damage model was possible to observe the influence of the concrete tensile behavior in the results, due to the significant shear component that occurred during the tests. Therefore, it is quite important the accurate simulation of the tensile behavior of reinforced concrete, to account for deformations due to shear effect. The numerical analysis through the fibers method allowed capturing the behavior of retrofit pier, PO2-N6-R1, once the model considers the behavior dominated by bending. The fiber model, which usually only take in account the bending failure mechanism, does not consider the piers web cracking due to shear and, therefore, cannot account for the stiffness degradation due to this piers cracking.

ACKNOWLEDGEMENT

The authors wish to acknowledge the “Irmãos Maia, Lda” company, for the construction of the tested piers and S.T.A.P.- Reparação, Consolidação e Modificação de Estruturas, S. A. company for the repair and retrofit works. Final acknowledgements to the laboratory staff, mainly Mr. Valdemar Luís, for all the care on the test preparation. This experimental tests were performed with the financial support of the “FCT- Fundação para a Ciência e Tecnologia" through the Project PTDC/ECM/72596/2006, ”Seismic Safety Assessment and Retrofitting of Bridges”.

REFERENCES

[1] R. Faria, J. Oliver, M. Cervera, A strain-based plastic viscous-damage model for massive concrete structures. *International Journal of Solids and Structures*, **35**(14), 1533-1558, 1998.

[2] P. Delgado, Avaliação da Segurança Sísmica de Pontes, FEUP: Porto, 2009. (in Portuguese) (http://ncrep.fe.up.pt/web/artigos/PDelgado_PhD_Thesis.pdf)

[3] R. Delgado, P. Delgado, N. Vila Pouca, A. Arêde, P. Rocha, A. Costa, Shear effects on hollow section piers under seismic actions: experimental and numerical analysis, *Bulletin of Earthquake Engineering*, **7**, 377-389, 2009 (DOI: 10.1007/s10518-008-9098-x).

[4] P. Delgado, A. Arêde, N. Vila Pouca, P. Rocha, A. Costa, R. Delgado, Retrofit of RC Hollow Piers with CFRP Sheets, *Composite Structures*, **94**, 1280–1287, doi:10.1016/j.compstruct.2011.11.032, 2012.

[5] P. Delgado, A. Monteiro, A. Arêde, N. Vila Pouca, R. Delgado, A. Costa, Numerical simulations of RC hollow piers under horizontal cyclic loading, *Journal of Earthquake Engineering*, **15**(6), 833-849, 2011.

[6] G.M. Calvi, A. Pavese, A. Rasulo, D. Bolognini, Experimental and Numerical Studies on the Seismic Response of R.C. Hollow Bridge Piers, *Bulletin of Earthquake Engineering*, **3:3**, 267-297, 2005.

[7] A. Pavese, D. Bolognini, S. Peloso, FRP seismic retrofit of RC square hollow section bridge piers, *Journal of Earthquake Engineering*, **1 SPEC. ISS**, 225-250, 2004.

[8] M.J.N. Priestley, F. Seible, G.M. Calvi, *Seismic design and retrofit of bridges*, New York: John Wiley & Sons, 1996.

[9] M.J. Kowalsky, Priestley, Improved Analytical Model for Shear Strength of Circular Reinforced Concrete Columns in Seismic Regions, *ACI Structural Journal*, **97:3**, 388-396, 2000.

[10] F. Sousa, Metodos de análise e avaliação de segurança sísmica de pontes em betão armado, MSc thesis, IPVC: Viana do Castelo, 2015. (in Portuguese) (waiting for publication).

[11] Seismosoft, SeismoStruct. computer program for static and dynamic nonlinear analysis of framed structures, 2006. Available online at: http://www.seismosoft.com.